Mahonia alkaloids (MA) ameliorate depression induced gap junction dysfunction by miR-205/Cx43 axis

Junhui He
  Guangxi Institute of Chinese Medicine & Pharmaceutical Science

Dongmei Li
  Guangxi Institute of Chinese Medicine & Pharmaceutical Science

Jie Wei
  Guangxi Institute of Chinese Medicine & Pharmaceutical Science

Sheng Wang
  The Center for Scientific Research of Anhui Medical University

Shifeng Chu
  Chinese Academy of Medical Sciences and Peking Union Medical College

Zhao Zhang
  Chinese Academy of Medical Sciences and Peking Union Medical College

Fei He
  Guangxi Institute of Chinese Medicine & Pharmaceutical Science

Dongmei Wei
  Guangxi Institute of Chinese Medicine & Pharmaceutical Science

Yi Li
  Guangxi Institute of Chinese Medicine & Pharmaceutical Science

Jiaxiu Xie
  Guangxi Institute of Chinese Medicine & Pharmaceutical Science

Guining Wei（✉ weiguining2013@163.com ）
  Guangxi Institute of Chinese Medicine & Pharmaceutical Science

Naihong Chen
  Chinese Academy of Medical Sciences and Peking Union Medical College

Research Article

Abstract

Depression has become an important disease threatening human health. In recent years, the efficacy of Traditional Chinese Medicine (TCM) in treating the disease has become increasingly prominent, so it is meaningful to find new antidepressant TCM. *Mahonia* fortune (Lindl.) Fedde is a primary drug in traditional formulas for the treatment of depression, however, the exact mechanism of its action is unclear. This study aimed to research the effect of MA on the improvement of gap junction function in depression via the miR-205/Cx43 pathway. The antidepressant effects of MA were observed by a rat model of reserpine-induced depression and a model of corticosterone (CORT)-induced astrocytes. The concentrations of neurotransmitters were measured by ELISA, the expression of Connexin 43 (Cx43) protein was measured by Immunohistochemistry, the expression of Cx43, BDNF, CREB proteins were measured by western-blot, the pathological changes of prefrontal cortex were observed by hematoxylin-eosin (H&E) staining. The binding of miR-205 and Cx43 was verified with a Luciferase reporter gene. Gap junction dysfunction detected by fluorescent yellow staining. The results confirmed that MA remarkably decreased miR-205 expression and increased Cx43, BDNF, CREB expression in depression rat and CORT-induced astrocytes. In addition, after overexpression of miR-205 *in vitro*, MA significantly increased Cx43, BDNF and CREB expression in CORT-induced astrocytes. Thus, MA may target Cx43 through miR-205 to regulate CREB/BDNF signaling pathway to improve depressive behavior.

Highlights

- *Mahonia* alkaloids (MA) ameliorate depression-like behavior of rats.
- MA ameliorate depression-like behavior by down-regulating miR-205 expression.
- GJA1 (Cx43) is a target gene of miR-205.
- MA regulate Cx43 protein.
- MA activate CREB/BDNF pathway to improve depression-like behavior through miR-205/Cx43.

Introduction

Depression is a global disease with high incidence, high mortality and high cost [1]. At present, there are 340 million depression patients in the world, and more than 26 million in China [2]. Despite a series of psychological and drug treatments for depression, only 74% of depression patients showed improvement [3]. Meanwhile, these drugs exhibit slow onset, side effects and limited efficacy, which in turn limit clinical application. Recently, TCM has drawn great attention on its potent effect for the treatment of depression, which exhibited low toxicity and high efficiency. However, there is an unmet need for novel TCM antidepressants with high efficiency and low toxicity.

The *Mahonia* belongs to the angiosperm phylum *Berberiaceae* [*Mahonia bealei* (Fort.) Carr.] and is a traditional medicinal plant in China [4]. Studies have shown that the chemical components contained in the *Mahonia* are mainly berberine, berberamine, rhizobine and palmatine [5]. Pharmacological studies

showed that the effects of *Mahonia* are antioxidant [6], anti-inflammatory [7] and antibacterial [8]. Our previous study showed that *Mahonia* have significant antidepressant effects, but the potential antidepressant mechanism is not yet clear.

MiRNAs are a class of approximately 22 nucleotide non-coding RNAs that functionally silence in a post-transcriptional manner [9, 10]. Many downstream target genes can be potentially regulate by miRNA through intracellular gene silencing mechanisms [11]. Studies have shown that miRNAs regulatory networks have an important role in the development of neuronal and function of brain [12, 13], and the importance of miRNAs for the regulation of brain function has been well elucidated, while more efforts are needed to understand in detail their pathological roles in neuropsychiatric disorders.

A host of studies revealed that Cx43 plays an important role in the process of depression, which could decrease the expression of Cx43 in human and rat [14–16]. Similarly, low expression of Cx43 induced depression in rat and mice [17]. Cx43 has the function of linking gap junctions with half connexins [18], and widely existed in nervous system. Furthermore, Cx43 is the main connexin of astrocyte [19]. Dysfunction of gap junctions and half connexins induced depressive behavior [20]. Therefore, the amelioration of the function of gap junctions is important for the regulation of depression.

In this study, we firstly explore the activity of antidepressant of *MA*. Then we detected the expression of miR-20a-5p, miR-186-5p, miR-205, miR-206, miR-382-3p, miR-495 in the brain tissue of depressive rat, and those genes related with depression were acquired by the Gene Expression Omnibus (GEO) database. The results showed that *MA* significantly decreased the expression of miR-205. Furthermore, we predicted the potential targets of miR-205 through TargetScan database (https://www.targetscan.org/vert_72/), the result shown that Cx43 has binding site with miR-205, and was verified in the HEK-293T and U251 cells. Finally, this study indicated that *MA* target Cx43 through miR-205 to regulate CREB/BDNF signaling pathway to improve depression. In short, our findings revealed that the antidepressant mechanism of *MA* is related with miR-205/Cx43 axis, this may be a hopeful target for *MA* and other TCM to the prevention or treatment in depression.

Method

Materials and reagents

Dried *Mahonia* were purchased form Guangxi Xianju Chinese Medicine Technology Co.. Acetonitrile (Nanning, Guangxi, China); methanol and formic acid were provided by Sigma (Sigma-Aldrich, USA); Fluoxetine was supplied by Lilly Suzhou Pharmaceutical Co., Ltd. (Suzhou, Jiangsu, China); The enzyme-linked immunosorbent assay (ELISA) kits for rat and human MAO, DA, NE, 5-HT were supplied by Shanghai Fanke Industrial Co., Ltd. (Shanghai, China); Lipofectamine 3000 and Trizol were provided by Invitrogen (USA); The PrimeScript RT Reagent Kit and SYBR Premix Dimer Eraser were provided by Vazyme Biotech Co., Ltd, (Nanjing, Jiangsu, China); The Mir-x miRNA First-Stand Synthesis Kit was purchased from TaKaRa (Japan); Anti-Cx43 and Anti-CREB were provided by Abcam (UK), Anti-p-CREB,

Anti-BDNF, GAPDH were provided by Wuhan Sanying Biotechnology Co., Ltd. (Wuhan, Hebei, China); Corticosterone (CORT) was provided by Aladdin (Shanghai, China).

Drug preparation

Dried *Mahonia* slices (500 g) were extracted 3 times with 5 L of water in a reflux system, combine the filtrate and concentrate into a paste. The thick paste was passed through silica gel column chromatography, recovered chloroform solution, concentrated, and obtained *MA* (3.22 g).

High-performance liquid chromatography (HPLC)

A UHPLC Dionex Ultimate 3000 (Thermo Scientific, San Jose, USA) equipped with a column oven and cooling autosampler was used. The separation was performed in a Supcrsil ODS C18 column (5.0 μm, 4.6 mm ×250 mm, Dalian Elite, China) with a column temperature maintained at 25 °C. The binary mobile solvents consisted of water containing 0.1% formic acid (v/v) (A) and acetonitrile (B) with the following gradient elution program: 0−40 min, 15−20% A; 40−60 min, 25−90% A; 60−70min, 90% A. The flow rate was 1.0 mL/min, the injection volume was 2 μL, and the split ratio was set at 1:1.

A Q-Exactive plus hybrid quadrupole-orbitrap mass spectrometer (Thermo Scientific, San Jose, USA) with a heat electrospray ionization (HESI) was employed. The mass conditions were as follows: spray voltage: + 4.0 kV; capillary temperature: 320 °C; auxiliary gas heater temperature: 300 °C; S-lens RF level: 50 V; by full MS/dd-MS2 scan mode: Scan range: 75-1125 m/z; Resolution: 70000; Automatic gain control (AGC) target: 1.0e5; Loop count: 5; Maximum injection time (IT): 50 ms; Isolation window: 2.0 m/z; Stepped NCE: 20, 40, 60; Apex trigger: 2-6 s; Dynamic exclusion: 10 s. Nitrogen was used for spray stabilization and as the collision gas in the C-trap. Q-Exactive 2.9 (Thermo Fisher Scientific, San Jose, USA) was used to control the mass spectrometer, Xcalibur 4.1 software (Thermo Fisher Scientific, San Jose, USA) was used to control the instrument and for data acquisition and analysis.

Animals

All of our experimental procedures conformed to internationally accepted principles for the use and care of experimental animals. The Animal Care Committee of the Institute of Chinese Medicine & Pharmaceutical Science approved the experiment. SD rats (180-220 g, 7-8 weeks), male, came from Changsha Tianqin Biotechnology Co., LTD. (Changsha, Hunan, China). All the animals were fed on a 12-hour daily/night cycle in an SPF level laboratory with a temperature of 25±1°C and humidity of 60±10%.

Reserpine-induced depression model protocol [21, 22]

The experiment rats were separated into normal, model (reserpine), positive (fluoxetine), *MA*-H and *MA*-L groups, with 10 rats in each group. The normal group was intraperitoneally injected with normal saline, and the other groups were intraperitoneally injected with 0.5 mg·kg^{-1}·d^{-1} reserpine for 10 days. The administration method is as follows when starting modeling: the positive group was given fluoxetine 1.8

mg·kg^{-1}, the *MA*-H group was assigned *MA* 2 mg·kg^{-1}, the *MA*-L group was assigned *MA* 1 mg·kg^{-1}, rats in normal group and model group were given an equal amount of distilled water intragastrically once a day.

Sucrose preference test

Water bottles of the same size, containing 1% sucrose water and drinking water, were administered simultaneously to the rats, and the bottles were withdrawn after 48 h of pre-adaptation. After 12 h of fasting and water deprivation, the consumption of 1% sucrose water and the consumption of drinking water was measured for 1 h. The percentage of sucrose water consumption was calculated. The ratio of sucrose water consumption was calculated.

Percentage of sucrose intake = [sugar water consumption / (sugar water consumption + drinking water consumption)] × 100%

Motion inhibition experiment

Placing the animals in the centre of a 40 cm diameter circular whiteboard and observed for 30 s. Record the time the rats stayed in the circle to observe motion inhibition of animals (mainly simulates reduced movement of animals in depressed state).

Cell culture

Human glioma cells U251 (Cell Bank of Chinese Academy of Sciences) were cultured in DMEM medium containing fetal bovine serum (10 %), penicillin and 100 ng/mL streptomycin (100 U·mL^{-1} and 100 ng·mL^{-1}). The cell lines were cultured in a 37 °C incubator with 5% CO_2.

CORT was dissolved with dimethyl sulfoxide (DMSO), and stored in a concentration of 50 mmol·L^{-1}. U251 cells were treated by CORT for 48 h in this research (simulation of CORT damage to astrocytes).

MA was dissolved with DMSO and stored in a concentration of 1 mg·mL^{-1}. U251 cells were pre-incubated by 200 μmol·L^{-1} CORT for 24 h, then treated by *MA* for 24 h and collected the cells.

Neurotransmitter detection

Pentobarbital sodium (2%, 0.3ml/100g) intraperitoneally, blood was obtained from the abdominal aorta and centrifuged for 10 min to collect serum. Culture supernatant of U251 cells were collected and centrifuged. The concentration of 5-HT, NE, DA were detected by ELISA kits.

Histopathological examination

Paraformaldehyde (4 %) were used to fix the brain tissues for 3 days, dehydrated and dewaxed, and then embedded in paraffin. The brain sections (3μm) were stained with H&E and observed under a light microscope at 20×. Analyzed images using the Image-Pro Plus 6.0 system.

Immunohistochemistry

The brain tissues were fixed with 4 % paraformaldehyde, dehydrated and dewaxed then embedded in paraffin. Staining was carried out after paraffin sections: the sections were baked in an oven for 4 hours at 60 °C, dewaxed with gradient ethanol, and then endogenous catalase was removed with 3% hydrogen peroxide. 5% bovine serum albumin (BSA) was blocked and incubated with primary antibody (Cx43, 1:100) at 4 °C overnight. After washing with phosphate-buffered saline (PBS) three times, the secondary antibody was incubated at room temperature 1 h, stained with 3,3 '- diaminobenzidine (DAB) and sealed. The analysis was performed using the image pro plus 6.0 system.

Relative quantitative real-time polymerase chain reaction (PCR) analysis

Total RNAs in U251 cells and hippocampus tissue were extracted by the TRIzol reagent. RNAs were reversed transcription by the PrimeScript RT Reagent Kit, miRNAs were reversed transcription by the Mir-x miRNA First-Stand Synthesis Kit. Quantitative RT-PCR was performed by the SYBR Premix Dimer Eraser on a LightCycler480II Real-Time PCR thermocycler (Roche, Switzerland). The primer of miR-205, miR-206-5p, miR-186, miR-186-5p, miR-20a-5p, miR-382-3p, miR-495, GJA1, GAPDH and U6 (Table 1) were compounded by the biological company. The $2^{-\Delta\Delta CT}$ relative quantitative method was used to normalize the results, and the internal control genes were U6 and GAPDH.

Table 1 The sequences of the primers for qRT-PCR

Name	Sequences (5'-3')	Size	species
miR-205-5p	TCCTTCATTCCACCGGAGTCTG	22	human
miR-205	TTCATTCCACCGGAGTCTGTAA	22	Rat
miR -206-5p	GCGGGCTTCTTTATATCCTCATA	23	Rat
miR -186	CAAGAATTCTCCTTTTGGGCTAA	23	human
miR -186-5p	TGGCTTCTCCTTTTGGGCTA	20	Rat
miR -20a-5p	GGGTGCTTATAGTGCAGGTAGAAA	24	Rat
miR -20a-5p	CGCGTAAAGTGCTTATAGTGCAGGTAG	27	human
miR -382-3p	AGGCATTCACGGACAACACTTA	22	Rat
miR -495	CAACAAACATGGTGCACTTCTTAA	24	Rat
GJA1-F	TGGTAAGGTGAAAATGCGAGG	21	human
GJA1-R	GCACTCAAGCTGAATCCATAGAT	23	human
U6-F	GGAACGATACAGAGAAGATTAGC	23	human
U6-R	TGGAACGCTTCACGAATTTGCG	22	human
GAPDH-F	GACAGCCGCATCTTCTTGTG	20	Rat
GAPDH-R	GAGAAGGCAGCCCTGGTAAC	20	Rat

Western blot analysis

The proteins of rat hippocampal tissue and U251 cells were extracted by adding 150 μL mixed lysate every 20 mg tissue, and a BCA protein assay was used to quantify the protein concentration. An equivalent denatured protein sample (100 μg) was added to each lane and separated by 12.5% sodium dodecyl sulfate-polyacrylamide gel electrophoresis and transferred onto polyvinylidene difluoride membranes[23, 24]. Seal the membrane with 5 % milk powder solution at room temperature for 1 hour, added primary antibody, and incubated in a shaking table at 4 °C overnight. Antibodies concentrations were Cx43 (1:1000), CREB (1:500), p-CREB (1:5000), BDNF (1:1000), GAPDH (1:5000). The membrane was washed slowly with TRIS-buffer brine (TBST) on an oscillator 3 times for 5 minutes each time. Then, an infrared fluorescent dye-labelled secondary antibody (1: 5000) was used to incubate the membranes. Finally, the membrane was washed 3 times with TBST. Image J software was used to analyze the grayscale, and the relative expression level of the protein was expressed by the ratio of the grayscale of the phosphorylated and unphosphorylated target bands.

Cytotoxicity Assays

The viability of U251 cells was detected with the help of the CCK-8 assay. Briefly, U251 cells were seeded into a 96-well plate with $1×10^4$ cell per well and treated by CORT or *MA*. After 24 or 48 h, 10 μL CCK-8 and 90 μL culture medium solution were added into each well. Then, the plate was placed at 37°C in incubator for 1 h. At last, the absorbance of each well was measured at 450 nm by Microplate Reader (Bioteck∐USA).

Dual-luciferase reporter assays

Lipofectamine 3000 were used to co-transfected the HEK-293T cells for miR-205 mimics or miR-NC and the Luciferase reporter plasmids. At 24 h post-transfection, the double Luciferase Reporter Assay system was used to analyze the double Luciferase activities. Luciferase activity was normalized to Renilla Luciferase activity.

pMIR-REPORTER (Ambion, CA, USA) vector was used to insert the 3'-UTRs of GJA1, predicted miR-205 seed matching sites and corresponding mutant sites after they were synthesized and annealed. In HEK-293T cells, a Dual-luciferase reporter assay was performed by co-transfected with wild-type plasmid or mutated reporter and miR-205 or miR-NC. 24 h after transfection, Luciferase activity was analyzed using a Dual-Luciferase Reporter Assay System (Promega, WI, USA).

Lucifer yellow staining

U251 cells were seeded into a 24-well plate with $20×10^4$ cell per well cultivated for 24 h in a 37 °C incubator with 5% CO_2, 0.05% Lucifer yellow 500 uL were added into per well, then, using a surgical blade, gently score the bottom of the plate with 3 parallel lines per well and continue incubation for 6 min, recycled dyes and added PBS 500 uL to fixed. Take photograph under a fluorescent microscope (Leica, Germany).

Statistical analysis

SPSS 22.0 (SPSS, Inc., Chicago, IL, USA) was used to analyze the data expressed as mean ± SD. All the data were analyzed by one-way analysis of variance (ANOVA) to determine the significance between the different groups. P-values of less than 0.05 were considered significant, where $*P < 0.05$, $**P < 0.01$.

Results

Chemical compounds in *MA*

As shown in figure 1, the typical chromatogram of *MA* by UHPLC/ESI Q-Orbitrap Mass Spectrometry analysis. It can be seen from the figure that *MA* contains more than 13 chemicals, and 8 chemical substances were identified by first and second mass spectrometry as well as literature and database search, and the results are showed in table 2.

Table 2 Identified chemical compounds in MA by UHPLC/ESI Q-Orbitrap Mass Spectrometry

Peak No.	R_t/min	Molecular formula	Product ions (m/z)	Identification
1	29.89	$C_{20}H_{24}NO_3^+$	303.64600, 234.86003, 188.08308, 137.05991, 116.68137	Unknow
2	32.16	$C_{20}H_{19}NO_4$	323.11469, 307.08347, 294.11118, 265.07343, 223.07343	Dihydroberberine
3	32.90	$C_{37}H_{43}O_5N_5^+$	573.55127, 297.16238, 162.09108	Unknow
4	33.68	$C_{20}H_{20}NO_4^+$	322.10672, 294.11191, 279.08853, 191.46196, 136.79010	Colunbamine
5	35.04	$C_{39}H_{45}N_2O_7^+$	545.07587, 441.31534, 282.16910, 227.10773, 174.09235	Unknown
6	36.84	$C_{20}H_{20}NO_4^+$	323.11484, 307.08310, 279.08926, 250.08717, 210.13094	Jatrorrhizne
7	37.51	$C_{39}H_{45}N_2O_7^+$	392.88751, 283.13419, 235.07533, 174.09126, 121.06539	Unknow
8	40.17	$C_{19}H_{16}NO_4^+$	307.08353, 292.05716, 279.08893, 250.08569, 212.44121	Berberrubine
9	43.51	$C_{21}H_{22}NO_4^+$	336.12238, 322.10746, 308.12723, 294.11139, 278.08139	Palmatine
10	43.56	$C_{20}H_{18}NO_4^+$	320.09131, 306.07565, 292.09647, 278.08051, 239.87100	Berberine
11	45.14	$C_{22}H_{24}NO_4^+$	350.13821, 322.14337, 308.12747, 278.11804	Dehydrocorydaline
12	47.17	$C_{21}H_{20}NO_4^+$	334.10681, 320.09042, 306.11203, 292.09637, 247.84787	Unknown
13	53.99	$C_{20}H_{17}NO_5$	337.09375, 322.07043, 308.09174, 294.07568, 279.05252	Oxyberberine

Effects of MA on reserpine-induced depression in rats

After with reserpine administered, compared with normal group, the sugar water intake (Fig. 2A) of model group was reduced ($P < 0.01$), yet the retention time in the circle (Fig. 2B) of model group was increased ($P < 0.01$), indicating that reserpine treatment induced depression-related behavior. Compared with model group, rats treated with MA exhibited a significantly increased the sugar water intake in MA-H ($P < 0.05$) and MA-L ($P < 0.05$) group; decreased retention time in the circle of MA-H ($P < 0.01$) and MA-L ($P < 0.01$).

Further, compared with normal group, the levels of 5-HT, DA and NE in model group were significantly decreased ($P < 0.05$, $P < 0.05$, $P < 0.05$), indicating that reserpine treatment induced a decrease in

neurotransmitter. Compared with model group, levels of 5-HT, DA and NE (Fig. 2C, 2D, 2E) in MA-H group were significantly increased ($P < 0.05$, $P < 0.01$, $P < 0.05$); but in MA-L group only 5-HT was significantly increased ($P < 0.05$). These data showed that treatment with MA improved depressive behaviors and neurotransmitter in rats.

Reserpine administration by intraperitoneal injection induced inflammtion in different brain regions of rats, with disorganized cell arrangement in the prefrontal cortex, sparse and enlarged intercellular matrix, and pyknosis of some nuclei, while MA significantly improved these pathological changes (Fig. 2F), indicating that MA improved inflammation in the prefrontal cortex of depression rats.

MA regulated miRNAs expression in depressive rats

The underlying antidepression molecular mechanisms of MA remain elucidated. Here, we measured the expression of miRNAs (miR-20a-5p, miR-186-5p, miR-206, miR-495, miR-382-3p, miR-205) associated with depression that selected by GEO database to observe if MA has effect on miRNA. The qRT-PCR results showed that miR-20a-5p, miR-186-5p and miR-205 (Fig. 3A, 3B, 3C) in brain tissues of depressive rats could significantly downregulated by MA ($P < 0.01$, $P < 0.05$, $P < 0.01$); miR-206 (Fig. 3D) was significantly upregulated by MA ($P < 0.01$); however, miR-382-3p and miR-495 (Fig. 3E, 3F) have no significant change by MA treatment ($P < 0.05$). The results indicated that MA regulated some miRNAs expression in depressive rats.

MA played an anti-depressive role in CORT-induced U251 cells

Next, we investigated the antidepressant mechanism of MA *in vitro*. Firstly, the effects of MA and CORT alone at different concentrations on the U251 cells were measured using the CCK-8 assay. The results showed that 24 h after MA treatment, the viability of U251 cells was significantly inhibited, and its IC_{50} was 200 µg·mL^{-1} (Fig. 4a); however, the viability of U251 cells treated with individual CORT for 24 h was no significant change (Fig. 4b), while 48 h after CORT treatment, the cell viability was significantly inhibited, and its IC_{50} was 200 µmol·L^{-1} (Fig. 4c).

Then, in order to find the appropriate concentration of CORT in depression models, we examined the expression of depression-related proteins CREB and BDNF by qRT-PCR. The results (Fig. 4d, 4e) showed that treatment with CORT 100 and 200 µmol·L^{-1} for 48 hours and MA 2 mg·kg^{-1} for 24 hours, CREB and BDNF levels were significantly decreased at 200 µmol·L^{-1} compared with normal group ($P < 0.01$, $P < 0.01$), while there was no significantly change of BDNF levels at 100 µmol·L^{-1}, indicating that CORT at 200 µmol·L^{-1} could successfully establish an in vitro model of depression. Compared with model group, treated with MA (2 mg·kg^{-1}) significantly increased CREB and BDNF levels in the two model groups ($P < 0.01$, $P < 0.01$). Therefore, CORT at 200 µmol·L^{-1} was chosen for modeling in subsequent experiments.

Further, the effect of MA on neurotransmitter in cell supernatant was measured by ELISA. In the results of Fig. 4f, 4g, 4h, compared with normal group, we observed decreased levels of 5-HT, DA and increased

levels of MAO in CORT-induced U251 cells supernatant ($P < 0.01$, $P < 0.01$, $P < 0.05$), while MA reversed these changes. These results implied that MA could alleviate the depressive effects caused by CORT on U251 cells.

Last, we detected the expressions of miR-205-5p, miR-186-5p and miR-20a-5p in CORT-induced U251 cells, which shown a significantly decreased by MA in depressive rats. The results (Fig. 4i, 4j) showed that the expression levels of miR-205-5p and miR-20a-5p in CORT-induced U251 cells were consistent with that in depressive rats, while miR-205-5p was the most significant different expressed.

GJA1 (Cx43) is a target gene of miR-205

To test whether miR-205 targets GJA1, GJA1 3'-UTR containing this seed sequence was cloned into pMIR-REPORTER vector (WT). Overexpression of miR-205 in HEK-293T cells decreased luciferase activities of wild type reporter to 70 %, suggesting that miR-205 inhibits its 3'-UTR reporter activities of GJA1. To test whether miR-205 specifically inhibits the activity by binding its seed sequence, we also made mutant construct with the mutation of miR-205 binding site in the 3'-UTR of GJA1 (Mut). Forced expression of miR-205 did not affect the transcriptional activation of mutant GJA1 3'-UTR reporter activity (Fig. 5b), indicating that miR-205 directly targets GJA1 by binding to its seed sequence at 3'-UTR. In addition, overexpression of miR-205 in U251 cells significantly suppressed Cx43 protein expression levels (Fig. 5d). These results indicated that GJA1 is a target gene of miR-205.

MA regulated Cx43 and CREB/BDNF pathway through miR-205 in CORT-induced U251 cells.

Next, the effects of MA on Cx43 and CREB/BDNF pathway were detected by western blotting. Compared with normal group, the results showed that the protein expression of Cx43, BDNF and p-CREB were significantly decreased in CORT-induced U251 cells ($P < 0.05$, $P < 0.05$, $P < 0.05$). Compared with model group, MA-H group significantly increased the expression of Cx43, BDNF and p-CREB ($P < 0.05$, $P < 0.05$, $P < 0.05$) (Fig. 6b, 6c, 6d). These results demonstrated that MA regulated Cx43 and CREB/BDNF signaling pathways.

In order to further verify whether MA regulated Cx43 and CREB/BDNF pathway through miR-205, miR-205 was overexpressed by miR-205 mimics in CORT-induced U251 cells. Compared with NC group, the expression of Cx43, BDNF and p-CREB were significantly decreased in miR-205 mimics group ($P < 0.01$, $P < 0.01$, $P < 0.01$), which were reversed by MA treatment (Fig. 6B, 6C, 6D). All these results provided evidence that MA played an anti-depressive role through miR-205 regulating Cx43 and CREB/BDNF pathway.

Effect of MA on Cx43 in the brain tissue of depressive rats

Finally, we investigated the effect of MA on Cx43 expression *in vivo*. The western blotting results (Fig. 7a, 7b) showed that the expression of Cx43 was significantly decreased in model group compared with normal group ($P < 0.01$). However, compared with model group, the expression of Cx43 was significantly increased with the administration of MA-H and MA-L group ($P < 0.01$, $P < 0.05$). Similar result

was observed in immunohistochemical detection (Fig. 7c, 7d). Evidently increased of Cx43 protein levels were found in MA-H and MA-L group relative to the model group ($P< 0.01$, $P< 0.01$). The above results demonstrated that MA improved depression by increased the level of Cx43 in brain tissue.

Effect of MA on CORT-induced gap junction dysfunction in U251 cells

Gap junction dysfunction is one of the manifestations of depression and can be measured by scrape-loading and dye transfer. As shown in Fig. 8, gap junction function was impaired in the model group, and the fluorescent dye could not be delivered outward from scratch through the intercellular gap junctions.
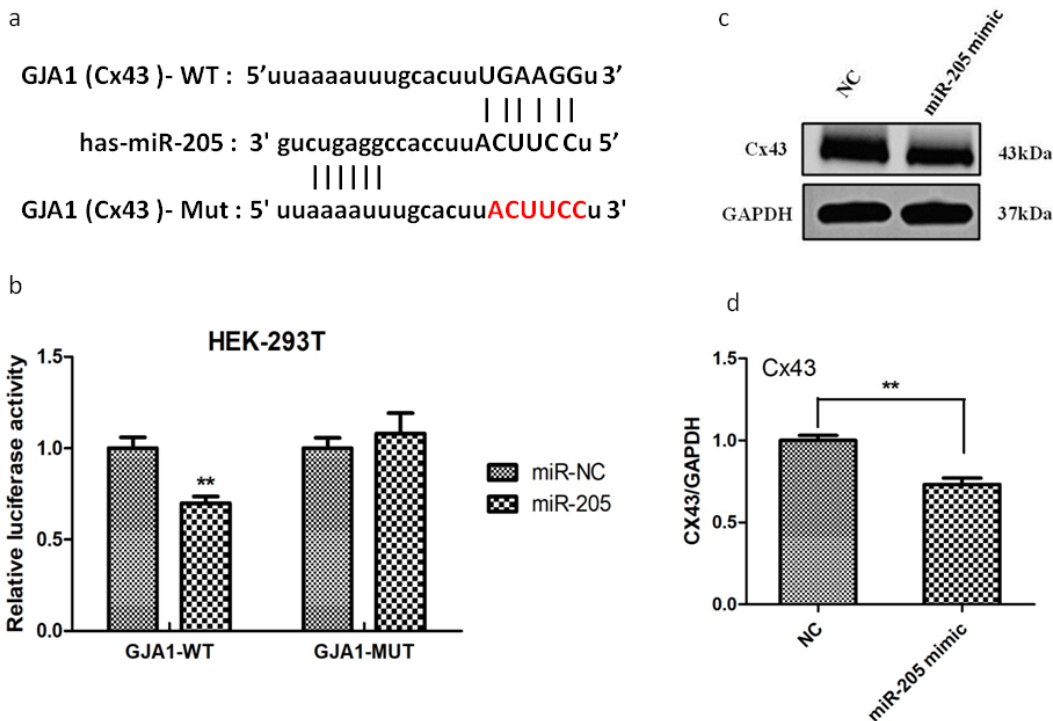
However, MA could enable the outward delivery of fluorescent dye, indicating that MA could improve CORT-induced intercellular gap junction dysfunction in astrocytes.

Discussion

In this study, we found that *MA* improved depression in reserpine-induced rats via miR-205 through the methods of ELISA, H&E staining, qRT-PCR and western-blotting, furthermore, the expression of Cx43 was increased after treatment with *MA* in the brain of depressive rats. Then, we overexpression miR-205 in vitro and found that *MA* played an anti-depressive role through miR-205 regulating Cx43 and CREB/BDNF pathway.

Studies have shown that Chinese herbal medicine can be used as supplements and substitutes for depression [25, 26]. There have been clinical trials to verify the effectiveness and safety of herbal therapies. The past few years, the mechanism of herbal medicines in treating depression has attracted significant attention [27]. *Mahonia* is a TCM herb, and in Anhui Herbal Medicine, it is described as clearing heat and detoxifying, detoxifying the liver and kidney; in Luchuan Materia Medica, it is described as cure febrile diseases, fever, upset, red eyes [28]. According to the TCM treatment of depression by draining the liver and relieving depression, warming the kidneys and strengthening the yang and the efficacy of *Mahonia*, we conducted an exploration of the antidepressant effects of its alkaloid components and found that it significantly increased sugar water preference and wilderness activity and improved depression-like behavior in rats.

Studies showed that miRNAs have an important regulatory role in the development of depression [29, 30]. In the present study, we found that *MA* downregulated miR-205 expression in depressed rat brain tissue

and CORT-induced U251 cells, indicating that the antidepressant effect of *MA* is closely related to miRNA. MiR-205 has been reported to be associated with the development of cervical cancer [31] and gastric cancer [32]. However, a single miRNA can often play a role in multiple diseases. In this study, we reported for the first time the association between miR-205 and depression and demonstrate that down-regulation of miR-205 improves depression.

Further, we searched the target of miR-205 through Bioinformatics Website, and found that Cx43 has binding site with miR-205. Interesting, Cx43 is the predominant gap junction protein in astrocytes and has been reported by numerous of studies that was closely associated with depression [33–35], but the mechanism of antidepression of miR-205 via Cx43 has not been reported. In the present study, CORT-induced astrocyte model was used to verify this result, which indicated that *MA* downregulated miR-205/Cx43 axis to ameliorate depression. Studies have shown that dysfunction of interstitial astrocyte gap junctions is an important pathogenesis of depression [36–38]. In this study, the result of fluorescent yellow dyeing confirmed of this view and revealed that *MA* could improve gap junction dysfunction in astrocytes.

BDNF is synthesized in neurons and glial cells, transported to terminals and released, and it plays an important role in neuronal maturation, synapse formation and synaptic plasticity in the brain. Studies have shown that the synergistic interactions between BDNF in neuronal activity and synaptic plasticity make it an ideal and important regulator of cellular processes that underlie cognition and other complex behaviors [39]. Whereas the CREB is an important transcription factor regulating BDNF and memory formation [40], the transcription factor CREB has been shown to play a key role in cognition and initiating memory integration [41, 42]. Gene expression mediated by CREB plays an important role in long-term memory, hippocampal neuroplasticity, dendritic growth, and neurogenesis [43]. In the present study, to observe the relationship between Cx43 and CREB/BDNF pathway, we examined their expression after administration of *MA* and overexpression of miR-205, respectively, and found that the expression of BDNF and CREB decreased in CORT-induced U251 cells, while the levels of both increased after *MA* treatment, indicating that *MA* has a role in regulating the CREB/BDNF pathway. In addition, the expression levels of BDNF and CREB increased after overexpression of miR-205 and administration of *MA* treatment, suggesting that *MA* may target Cx43 via miR-205 to regulate the CREB/BDNF pathway and improve depression.

Conclusions

In conclusion, the antidepressant effect of *MA* was associated with downregulation of miR-205 expression, and upregulation of Cx43, CREB and BDNF. *MA* improved depression by inhibiting miR-205, elevating Cx43 levels and activating CREB/BDNF pathway. *MA* could be investigated as a potential complementary drug for depressed patients. In addition, follow-up studies on the effects of *MA* on neuroplastic function and other molecular mechanisms of depression are currently underway to develop *MA* as an effective agent for the successful treatment of depression.

Declarations

Disclosure Statement

The authors declare no conflicts of interest associated with this study.

References

1. Shi, Z., S. Xiao, and X. Li, *Treatment resistant depression or dementia: a case report.* Shanghai Arch Psychiatry, 2016. **28**(2): p. 109-14.
2. Packnett, E.R., et al., *Epidemiology of Major Depressive Disorder Disability in the US Military: FY 2007-2012.* J Nerv Ment Dis, 2017. **205**(9): p. 672-678.
3. McHugh, R.K., et al., *Patient preference for psychological vs pharmacologic treatment of psychiatric disorders: a meta-analytic review.* J Clin Psychiatry, 2013. **74**(6): p. 595-602.
4. Yu, T., W. Su, and L. Rong, *Research progress of Mahonia (Berberidaceae).* Journal of Guizhou Normal University (Natural Sciences), 2015. **33**(3): p. 115-120.
5. KJ, H., L. BM, and L. WJ, *Chemical constituents from Mahonia duclouxiana Gagnep.(I).* West China Journal of Pharmacy, 2008. **23**(2): p. 172-173.
6. Hong L, et al., *Advances in Chemical Composition，Pharmacological Action and Quality Control of Mahonia bealei. .* Guizhou Agricultural Sciences, 2019. **9**(47): p. 122-125.
7. Li YJ, et al., *Long columns and broad-leaved Mahonia Mahonia Comparative pharmacological effects of aqueous extract.* Guiding Journal of Traditional Chinese Medicine and Pharmacy, 2010. **16**(9): p. 92-96.
8. Li YJ, et al., *Comparison of pharmacological effects of ethanol extracts from Mahonia longzhuensis and Mahonia broadleaf.* Yunnan Journal of traditional Chinese Medicine, 2010. **31**(8): p. 61-63.
9. Nadim, W.D., et al., *MicroRNAs in Neurocognitive Dysfunctions: New Molecular Targets for Pharmacological Treatments?* Curr Neuropharmacol, 2017. **15**(2): p. 260-275.

10. Rajman, M. and G. Schratt, *MicroRNAs in neural development: from master regulators to fine-tuners.* Development, 2017. **144**(13): p. 2310-2322.

11. Cao, T. and X.C. Zhen, *Dysregulation of miRNA and its potential therapeutic application in schizophrenia.* CNS Neurosci Ther, 2018. **24**(7): p. 586-597.

12. Winter, J., et al., *Many roads to maturity: microRNA biogenesis pathways and their regulation.* Nat Cell Biol, 2009. **11**(3): p. 228-34.

13. Bartel, D.P., *MicroRNAs: genomics, biogenesis, mechanism, and function.* Cell, 2004. **116**(2): p. 281-97.

14. Wang, H., et al., *Ginsenoside Rg1 Ameliorates Neuroinflammation via Suppression of Connexin43 Ubiquitination to Attenuate Depression.* Front Pharmacol, 2021. **12**: p. 709019.

15. Xia, C.Y., et al., *Connexin 43: A novel ginsenoside Rg1-sensitive target in a rat model of depression.* Neuropharmacology, 2020. **170**: p. 108041.

16. Wang, H.Q., et al., *Novel antidepressant mechanism of ginsenoside Rg1: Regulating biosynthesis and degradation of connexin43.* J Ethnopharmacol, 2021. **278**: p. 114212.

17. Zhang, N.N., et al., *Connexin 43: insights into candidate pathological mechanisms of depression and its implications in antidepressant therapy.* Acta Pharmacol Sin, 2022.

18. Delvaeye, T., et al., *Therapeutic Targeting of Connexin Channels: New Views and Challenges.* Trends Mol Med, 2018. **24**(12): p. 1036-1053.

19. Chen, J., et al., *Effects of chronic mild stress on behavioral and neurobiological parameters - Role of glucocorticoid.* Horm Behav, 2016. **78**: p. 150-9.

20. Xia, C.Y., et al., *A novel mechanism of depression: role for connexins.* Eur Neuropsychopharmacol, 2018. **28**(4): p. 483-498.

21. Zong, Y., et al., *Si-Ni-San Prevents Reserpine-Induced Depression by Inhibiting Inflammation and Regulating CYP450 Enzymatic Activity.* Front Pharmacol, 2019. **10**: p. 1518.

22. Tang, Y.Q., et al., *Venlafaxine plus melatonin ameliorate reserpine-induced depression-like behavior in zebrafish.* Neurotoxicol Teratol, 2019. **76**: p. 106835.

23. Chen, W.-F., et al., *Neuroprotective properties of icariin in MPTP-induced mouse model of Parkinson's disease: Involvement of PI3K/Akt and MEK/ERK signaling pathways.* Phytomedicine, 2017. **25**: p. 93-99.

24. Ye, F., et al., *The regulatory mechanisms of Yulangsan MHBFC reversing cardiac remodeling in rats based on eNOS-NO signaling pathway.* Biomedicine & Pharmacotherapy, 2019. **117**: p. 109141.

25. Zhang, C., et al., *Urinary metabonomics study of anti-depressive mechanisms of Millettia speciosa Champ on rats with chronic unpredictable mild stress-induced depression.* J Pharm Biomed Anal, 2021. **205**: p. 114338.

26. Zhang, H., et al., *Integrated analysis of the chemical-material basis and molecular mechanisms for the classic herbal formula of Lily Bulb and Rehmannia Decoction in alleviating depression.* Chin Med, 2021. **16**(1): p. 107.

27. Wang, Y., et al., *Chinese Herbal Medicine for the Treatment of Depression: Applications, Efficacies and Mechanisms.* Curr Pharm Des, 2017. **23**(34): p. 5180-5190.

28. Lu, X., *Mahonia of the whole plant.* Forestry of Guangxi 2015. **7**: p. 21-22.

29. Fiori, L.M., et al., *miR-323a regulates ERBB4 and is involved in depression.* Mol Psychiatry, 2020.

30. Yoshino, Y., B. Roy, and Y. Dwivedi, *Altered miRNA landscape of the anterior cingulate cortex is associated with potential loss of key neuronal functions in depressed brain.* Eur Neuropsychopharmacol, 2020. **40**: p. 70-84.

31. Liu, J., et al., *Upregulation of miR-205 induces CHN1 expression, which is associated with the aggressive behaviour of cervical cancer cells and correlated with lymph node metastasis.* BMC Cancer, 2020. **20**(1): p. 1029.

32. Xian, X.S., Y.T. Wang, and X.M. Jiang, *Propofol Inhibits Proliferation and Invasion of Stomach Cancer Cells by Regulating miR-205/YAP1 Axis.* Cancer Manag Res, 2020. **12**: p. 10771-10779.

33. Shen, F., et al., *Genistein Improves the Major Depression through Suppressing the Expression of miR-221/222 by Targeting Connexin 43.* Psychiatry Investigation, 2018. **15**(10): p. 919-925.

34. Morioka, N., et al., *Decreased connexin43 expression in the hippocampus is related to the antidepressant effect of amitriptyline in neuropathic pain mice.* Biochem Biophys Res Commun, 2021. **566**: p. 141-147.

35. Zhang, Y., et al., *Xiaoyao powder alleviates the hippocampal neuron damage in chronic unpredictable mild stress-induced depression model rats in hippocampus via connexin 43Cx43/glucocorticoid receptor/brain-derived neurotrophic factor signaling pathway.* Bioengineered, 2022. **13**(1): p. 383-394.

36. Xia, C.Y., et al., *Corticosterone impairs gap junctions in the prefrontal cortical and hippocampal astrocytes via different mechanisms.* Neuropharmacology, 2018. **131**: p. 20-30.

37. Ren, Q., et al., *Gap junction channels as potential targets for the treatment of major depressive disorder.* Psychopharmacology (Berl), 2018. **235**(1): p. 1-12.

38. Sun, J.D., et al., *Gap junction dysfunction in the prefrontal cortex induces depressive-like behaviors in rats.* Neuropsychopharmacology, 2012. **37**(5): p. 1305-20.

39. Bjorkholm, C. and L.M. Monteggia, *BDNF - a key transducer of antidepressant effects.* Neuropharmacology, 2016. **102**: p. 72-9.

40. Rosa, E. and M. Fahnestock, *CREB expression mediates amyloid beta-induced basal BDNF downregulation.* Neurobiol Aging, 2015. **36**(8): p. 2406-13.

41. Lee, Y.S. and A.J. Silva, *The molecular and cellular biology of enhanced cognition.* Nat Rev Neurosci, 2009. **10**(2): p. 126-40.

42. Kaldun, J.C. and S.G. Sprecher, *Initiated by CREB: Resolving Gene Regulatory Programs in Learning and Memory: Switch in Cofactors and Transcription Regulators between Memory Consolidation and Maintenance Network.* Bioessays, 2019. **41**(8): p. e1900045.

43. Todorovski, Z., et al., *LIMK1 regulates long-term memory and synaptic plasticity via the transcriptional factor CREB.* Mol Cell Biol, 2015. **35**(8): p. 1316-28.
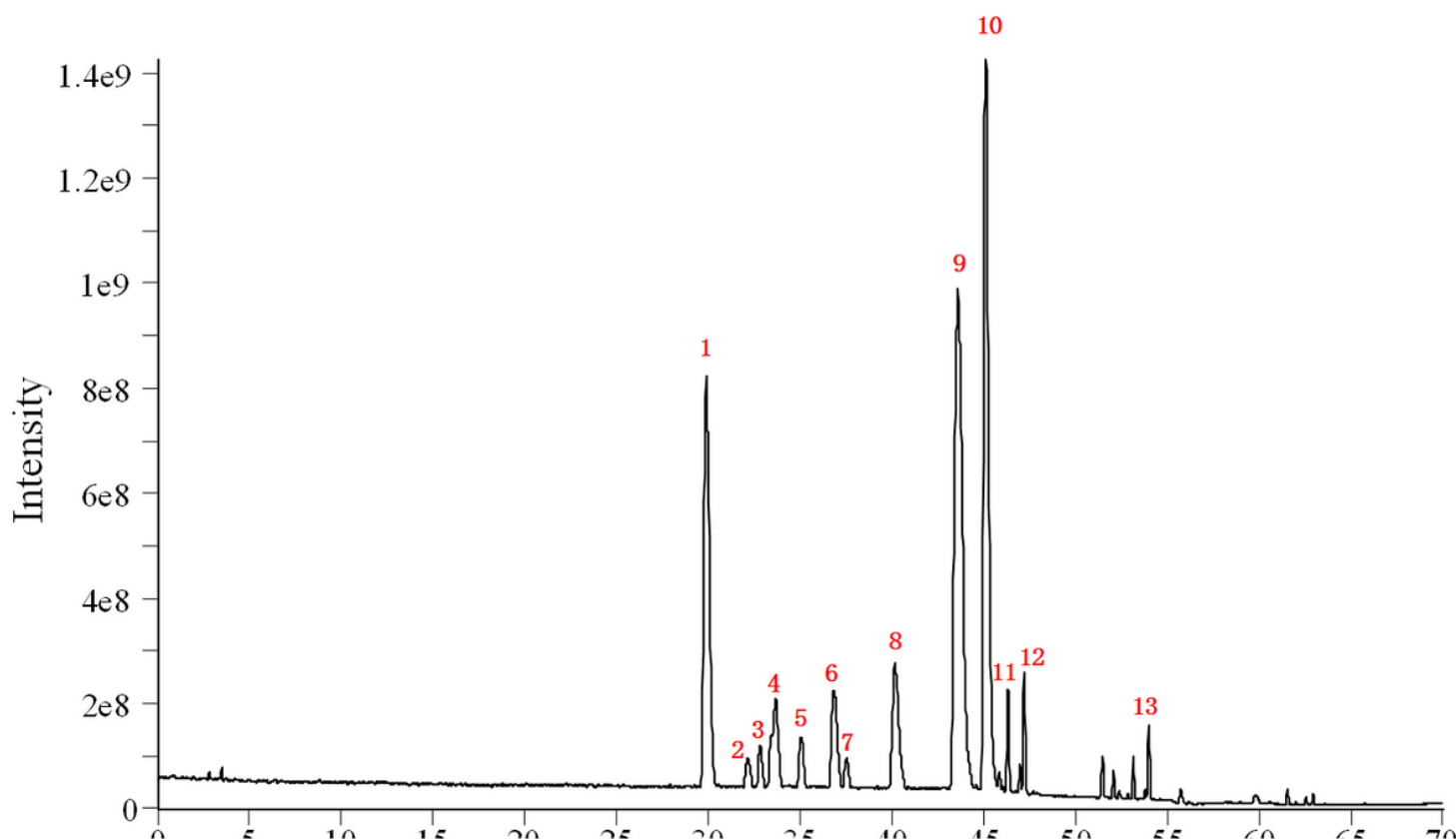
Figures

Figure 1

The typical chromatogram of MA by UHPLC/ESI Q-Orbitrap Mass Spectrometry analysis

Figure 2

Effects of MA on reserpine-induced depressive behaviors, neurotransmitters and inflammatory infiltration of prefrontal cortex in rats. A: sucrose preference (%); B: in-circle retention (s); C: The concentration of 5-HT (ng/mL); D: The concentration of DA (ng/mL); E: The concentration of NE (ng/mL); F: HE staining (20´). Data are expressed as the mean ± SD (n=6). #$P < 0.05$, ##$P < 0.01$ compared to the normal group, *$P < 0.05$, **$P < 0.01$ compared to the model group.
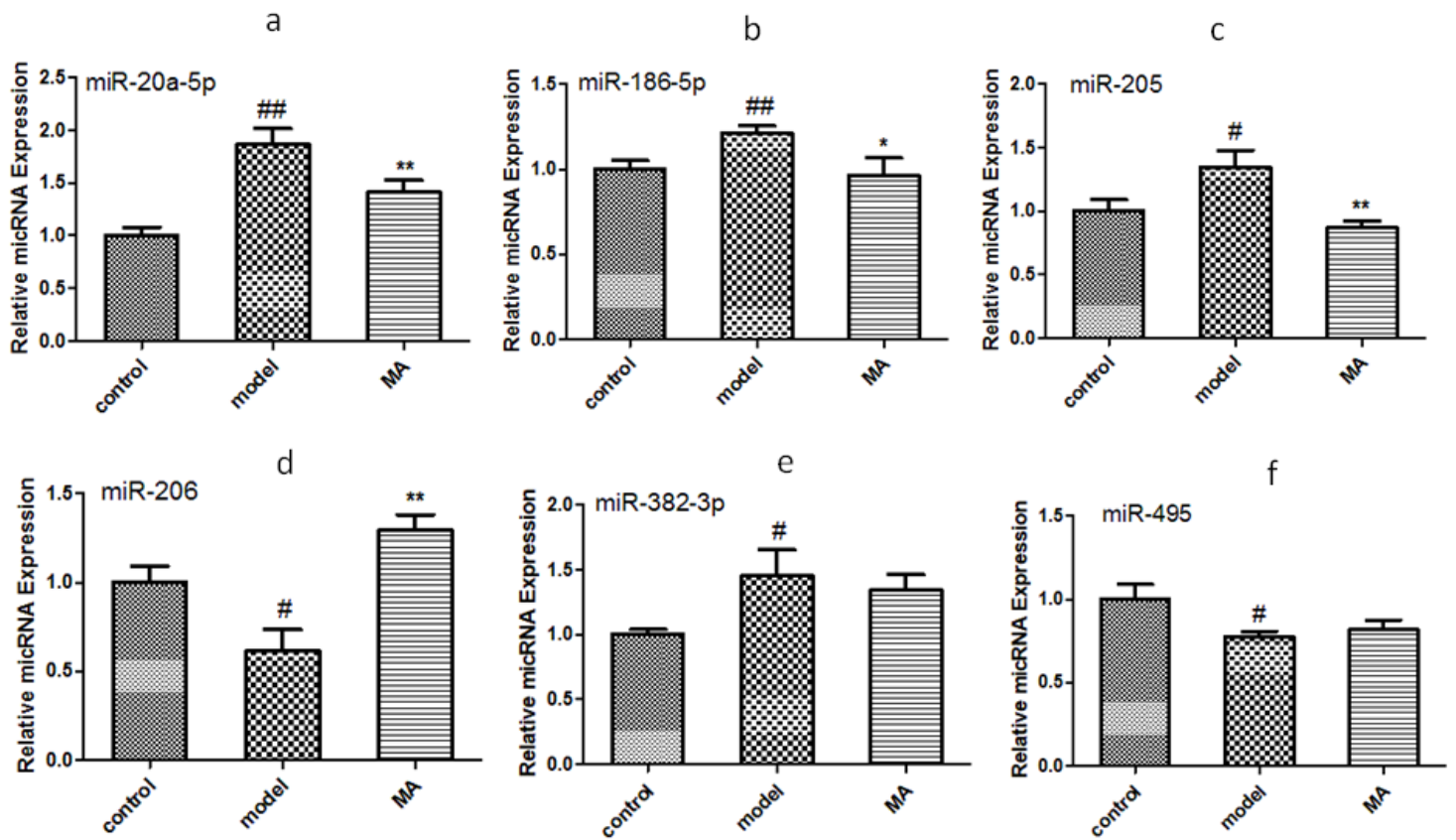
Figure 3

MA regulated miRNAs expression in depressive rats. A: Relative miR-20a-5p expression; B: Relative miR-186-5p expression; C: Relative miR-205 expression；D: Relative miR-206 expression; E: Relative miR-382-3p expression; F: Relative miR-495 expression. Data are represented as the mean ± SD (n=3). #*P* < 0.05, ##*P* < 0.01 compared to the normal group, *P* < 0.05, **P* < 0.01 compared to the model group.

Figure 4

MA played an anti-depressive role in CORT-induced U251 cells. a: Cell viability after 24h of MA action(%); b: Cell viability after 24h of CORT action(%); c: Cell viability after 48h of CORT action(%); d: Relative CREB mRNA expression after administration of different concentrations of CORT modeling and 2 mg/mL MA treatment; e: Relative BDNF mRNA expression after administration of different concentrations of CORT modeling and 2 mg/mL MA treatment; f: The concentration of 5-HT (pg/mL); g: The concentration of DA (nmol/L); h: The concentration of MAO (ng/mL); i: Relative expression of miR-186-5p; j: Relative expression of miR-205; k: Relative miR-20a-5p expression. Data are represented as the mean ± SD (n=6 or n=3). #*P* < 0.05, ##*P* < 0.01 compared to the normal group, *P* < 0.05, **P* < 0.01 compared to the model group.

Figure 5

GJA1 (Cx43) is a target gene of miR-205. a: miR-205 and GJA1 binding site prediction. b: Luciferase activity in Luciferase reporter gene assay. c: Western Blot strip. d: Cx43/GAPDH. Data are represented as the mean ± SD (n=3). #P< 0.05, ##P< 0.01 compared to the normal group, *P< 0.05, **P< 0.01 compared to the model group.

Figure 6

MA regulated Cx43 and CREB/BDNF pathway through miR-205 in CORT-induced U251 cells. a: Western Blot strips; b: Cx43/GAPDH; c: BDNF/GAPDH; d: p-CREB/CREB; e: Western Blot strips (overexpress); f: Cx43/GAPDH (overexpress); g: BDNF/GAPDH (overexpress); h: p-CREB/CREB (overexpress). Data are represented as the mean ± SD (n=3). #P< 0.05, ##P< 0.01 compared to the normal group, *P< 0.05, **P< 0.01 compared to the model group.

Figure 7

Effect of MA on Cx43 in the brain tissue of depressive rats. a: WB strips; b: Cx43/GAPDH; c: Immunohistochemistry results of Cx43 protein (20×); d: Positive expression rate of Cx43 (%). Data are represented as the mean ± SD (n=3 or n=5). #P< 0.05, ##P< 0.01 compared to the normal group, *P< 0.05, **P< 0.01 compared to the model group.

Figure 8

Effect of MA on CORT-induced gap junction dysfunction in U251 cells. a: normal group; b: model group; c:MA-H group; d: MA-L group (10×).

Supplementary Files

This is a list of supplementary files associated with this preprint. Click to download.

- QualitativeAnalysisReportofMahoniaalkaloids.docx
- GraphicalAbstract.png